INTERNATIONAL JOURNAL OF OPTIMIZATION IN CIVIL ENGINEERING
Int. J. Optim. Civil Eng., 2021; 11(3): 461-479

OPTIMAL DESIGN OF THE IMPACT DAMPER IN FREE VIBRATIONS OF SDOF SYSTEM USING ICACO

H. Safaeifar[1*, †] and M. Sheikhi Azqandi[2]
[1]*Mechanical Engineering Department, Bozorgmehr University of Qaenat, Qaen, Iran*
[2]*Mechanical Engineering Department, University of Birjand, Birjand, Iran*

ABSTRACT

The impact damper is a passive method for controlling vibrations of dynamic systems. It is designed by placing one or several masses in a container, which is installed on the structure. Damping performance is affected by many parameters, such as the mass ratio of the primary structure, size, number, and material of the particles, friction and restitution coefficients of the particles and gap distance. Impact damper is effective, economical, and practical and its functionality can be further enhanced by an optimal design. In this paper, first, the mathematical modeling of a rigid impact damper used in free vibration reduction of a single degree of freedom (SDOF) system is performed. The results on this step are validated with those results of previous studies, and a good agreement is achieved. Next, the robust hybrid optimization method that is called Imperialist Competitive Ant Colony Optimization (ICACO) is introduced. After that, the damper function is optimized using ICACO, and the optimum values of the effective parameters for maximizing damping effectiveness are obtained. Comparing the results of the optimized and the basic designs shows that the optimization method is robust and the optimal results are practical. The optimum design of damper parameters using ICACO method can damp more than %94 of the system's initial energy in a short time.

Keywords: optimal design; free vibration; energy damping; impact damper; hybrid optimization method.

Received: 17 June 2021; Accepted: 5 August 2021

1. INTRODUCTION

The impact damper (ID) is an effective passive method for controlling vibrations of dynamic

---

*Corresponding author: Mechanical Engineering Department, Bozorgmehr University of Qaenat, Qaen, Iran
†E-mail address: safaeifar@buqaen.ac.ir (H. Safaeifar)

systems especially in civil infrastructure systems, the aerospace structures, and machinery fields [1-2]. The experimental and analytical works on the performance of the impact dampers show that these non-linear dampers have a better performance than the linear vibration dampers in decreasing the oscillations of structures [3-7].

The impact damper has a container with one or several auxiliary masses (particles). When the primary structure vibrates, its kinetic energy is transferred to the masses, which then impact each other and the container. Therefore, the kinetic energy of the primary structure is decreased [8]. The auxiliary masses decrease the vibrations of the primary system by the impacts, which is why the damper is called the impact dampers. To increase the functionality, impact dampers are installed where the vibration amplitude of the structure is maximum [9]. The impact dampers are divided into rigid and resilient types. The impact period in the rigid type is assumed to be very short and so, the displacement of masses at the impact time is neglected. The displacement of masses is considered in the resilient damper [10]. The rigid body dynamics govern the rigid damper analysis, while the contact force model must be considered in a resilient impact. The contact force models were presented by Flores et al [11], Hu and Guo [12] and Safaeifar and Farshidianfar [13].

Impact dampers display a number of advantages. They are especially valuable in harsh conditions, negligibly sensitive to oil contamination, and have a low weight impact [1]; can operate in multiple directions and at a wide domain of frequencies [14]; are not sensitive to the ambient temperature [15,16]; can be worked without any origin of power; create to have low sensitivity to excitation in directions other than the principal one [17]; do not hurt from wear [16,18]; are effective at damping either random, Gaussian, or deterministic excitation [19]; and, are highly reliable, simple, and affordable [18]. These characteristics make them especially valuable in harsh environments, in situations where hydraulic or electric power cannot be transmitted, and where vibrations are chaotic [20].

Masri, introduced the single-mass impact damper in 1965, for the first time, and evaluated its functionality experimentally and analytically [21]. The results of this research show that the impact damper can significantly decrease the response domain of vibrational systems in harmonic, sudden, and shock loads provided that the design parameters are adjusted correctly. Masri also evaluated the application of a multi-unit impact damper in free vibrations of a single-DOF system [22]. His research discovered that the efficiency of the multi-unit damper in reducing the vibration amplitude is much higher than the single-unit damper. The application of impact dampers in the steady-state response of multi-DOF vibration systems is studied by Masri [23]. His research showed that the impact damper is an effective mechanism in reducing the vibrations of multi-DOF systems like tall buildings.

Bapat and Sankar studied the application of a single-mass impact damper in free and forced vibrations of an SDOF system [24]. One of the most important results of this work is determining the optimum gap distance for improving the damper performance. This gap distance was not obtained using optimization methods, but got only by comparing the system response in different conditions.

Ema and Marui conducted a fundamental study on the single-mass impact damper [25]. In this research, the optimum damping is achieved by adjusting the mass ratio and the gap distance properly. Afsharfard and Kolahan studied the behavior of single-mass impact dampers based on the reliability factor [26]. They obtained the variation of the system's damping and reliability with the coefficient of restitution. Li et al [27] discussed on the effects of different parameters that will have an influence on the performance of the impact damper.

Based on experimental and theoretical studies performed by researchers all over the world, it has been confirmed that the impact damping technology has great superiority in vibration attenuation control encountered in the civil engineering field [1]. Lu et al [6] proposed a performance-based optimal design method of the impact damper system. Zurawski and Zalewski [28] studied the vibrations of beams which were damped by using tuned particles impact damper. Ozbulut et al [29] determined the vibration reduction ratio of a 20-story nonlinear benchmark structure with a new re-centering variable friction device. Rana and Soong invented an impact damper for a single degree of freedom structure and a certain vibration mode of a multi-degree of freedom by optimization method and reviewed the controlling of multiple structural vibration modes [30]. Bakre et al determined equations of optimal parameters for impact dampers utilized to a single degree of freedom main system for various excitations and objective functions, such as dynamic displacement, velocity, and base shear [31]. In addition, some meta-heuristic optimization methods such as genetic algorithm [32], particle swarm optimization [33], bionic algorithm [34], differential evolution algorithm [6], harmony search algorithm [35-36], and whale optimization algorithm [37] have been introduced to design the optimum parameters for the impact damping system.

The literature review on the application of impact dampers in SDOF free vibration systems shows that the effects of different parameters, including mass ratio, coefficient of restitution, and gap distance are investigated in most studies. The selection of parameters was typically performed by comparing the obtained results and rarely using optimization methods. In addition, the randomness, and nonlinearity of the impact damping are two major difficulties and there have been no corresponding theories to describe these two complex highly nonlinear phenomena appropriately up to now [1].

For this purpose, at the present paper, a meta-heuristic optimization method is used due to the complexity and high computational cost of the problem.

In the last two decades, metaheuristic optimization methods, due to their superior benefits, have been noticed much for the analysis of engineering optimization problems. In these methods, there is no need for derivability or continuously of the objective function and in addition, they are more likely to converge to the global optimal point [38]. Imperialist Competitive Ant Colony Optimization (ICACO) is a hybrid robust metaheuristic optimization method which has great advantages including easy performance, the low number of tunning parameters, high ability to the analysis of complex engineering problems and, fast convergence rate [39].

The performance optimization of impact dampers in SDOF vibrations systems is studied in this paper and optimum values of mass ratio, coefficient of restitution, and gap distance are determined. First, the mathematical modeling of the impact damper used in free vibration analysis of the SDOF system is conducted. Then, optimization method ICACO is introduced. Next, the damper performance in the system is optimized. Finally, the optimization results are presented and conclusions are provided.

2. MATHEEMATICAL MODELING

The model presented in Fig. 1 is used for evaluating the impact damper performance in an SDOF vibration system.

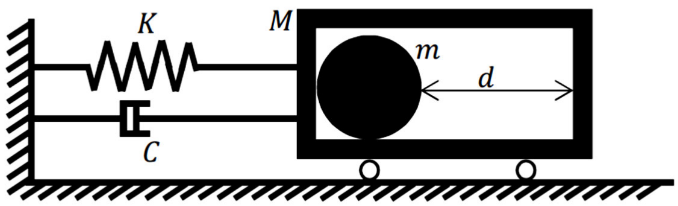

Figure 1. Simplified model for SDOF system

The equation of motion for the primary and the auxiliary systems is given by Eqs. (1) and (2) respectively. At these equations are assumed that there is no collision between them [40]:

$$M\ddot{x}_M + C\dot{x}_M + Kx_M = 0 \tag{1}$$
$$m\ddot{x} = 0 \tag{2}$$

where *M*, *C*, and *K* are mass, damping, and stiffness of the primary system, respectively, and *m* is mass of the auxiliary system. x_M and x are the responses of the primary and auxiliary systems, respectively. The center of the container in its initial state is considered as the origin. The responses are given by Eqs. (3) and (4).

$$x_M(t) = e^{-\xi\omega_n t}\left(x_{0M}\cos\big(\omega_d\,(t-t_0)\big) + \frac{V_{0M} + \xi\,\omega_n\,x_{0M}}{\omega_d}\sin\big(\omega_d\,(t-t_0)\big)\right) \tag{3}$$
$$x(t) = V_0(t-t_0) + x_0 \tag{4}$$

where ξ , w_n, and w_d are the damping ratio, undamped natural frequency, and damped natural frequency of the primary system, respectively, and are given by Eqs (5) to (7):

$$\xi = C/\big(2\sqrt{KM}\big) \tag{5}$$
$$\omega_n = \sqrt{K/M} \tag{6}$$
$$\omega_d = \left(\sqrt{1-\xi^2}\right)\omega_n \tag{7}$$

where t_0 is the impact time of the auxiliary system with left or right wall. x_{0M} , V_{0M} , x_0 and V_0 are the location and the velocity of the primary and auxiliary systems immediately after each impact, respectively. When the auxiliary system impacts with the left or right walls, the required conditions are given by Eq. (8) and Eq. (9), respectively. *d* is the gap distance.

$$x - (x_M - d/2) = 0 \tag{8}$$
$$(x_M + d/2) - x = 0 \tag{9}$$

Assuming two impacting masses are rigid and the impact time is very short, the location of these masses remains unchanged instantly after the impact. However, their velocity is changed. The new velocities can be calculated based on the linear momentum conservation and the coefficient of restitution. For the collision of two systems with masses *M* and *m,* their new velocities are given by Eq. (10) and Eq. (11), respectively [41].

$$V_1{}' = \frac{(1-\mu e)V_1 + \mu(1+e)V_2}{1+\mu} \tag{10}$$

$$V_2{}' = \frac{(1+e)V_1 + (\mu - e)V_2}{1+\mu} \tag{11}$$

where e and $\mu = m/M$ are coefficients of restitution and mass ratio in the head-on collision of two bodies, respectively. V_1 and V_2 are velocities of two masses before the collision, and V_1' and V_2' are velocities of two masses after the collision.

It should be reminded that the locations of the primary and the auxiliary systems after each collision, x_0, and x_{0M}, are equal to the corresponding values just before the collision. The velocities of two masses after each collision are obtained using Eqs. (10) and (11).

To verify the current model, the results are compared with the results of Bapat and Sankar [24]. The utilized data are given in Table 1.

Table 1: Numerical values used to evaluate single-mass impact damper [24]

	Parameter	Value
M	Mass of main system	281.25 gr
K	Stiffness of main system	1026.39 N/m
C	Damping of main system	0.1359 Ns/m
m	Impact Mass	11.90 gr
e	Coefficient of restitution	0.4
d	Gap distance	9.5 mm
x_{0M}	Initial displacement of main mass	12.7 mm
V_{0M}	Initial velocity of main system	0 mm/s

After using the input parameter from Table 1 in the written code, the comparison of the variation of vibration amplitude during the time for an SDOF system with a single-mass impact damper between present research and Bapat and Sankar research [24] is given in Fig. 2.

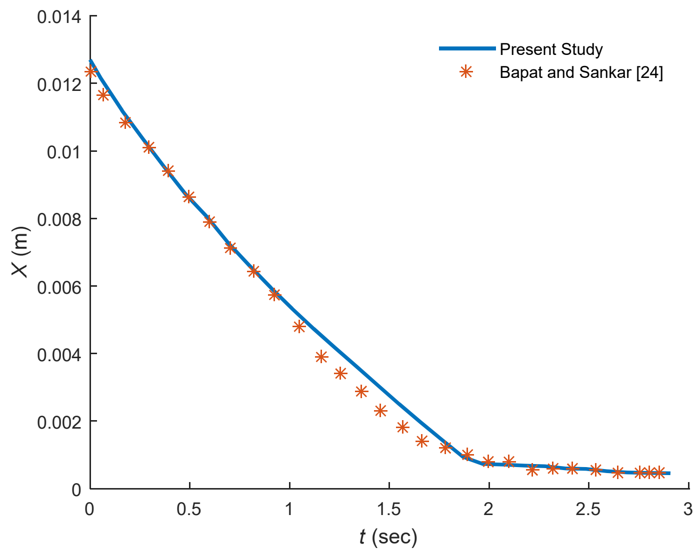

Figure 2. Evaluation of single-mass impact damper

As observed, there is an excellent agreement between the two results. Therefore, the optimization of the model can now be carried out.

3. OPTIMIZATION PROCEDURE

3.1 Imperialist competitive algorithm (ICA)

Imperialist competitive algorithm is a robust optimization technique using socio-political mutation of humans as a source of inspiration. The initial population at ICA produces randomly and each individual of them is named 'country'. These countries are divided into two groups, including imperialists and colonies of imperialists. Colonies are under the ownership of an imperialist. The imperialists have much authority (the more optimized countries) with respect to colonies so all the colonies are divided between imperialists based on the authority of them. Each empire is included an imperialist with its colonies. During the optimization procedure, colonies begin to move to its imperialist. In an empire, if a colony has a better authority than that of an imperialist, the position of the colony and its associated imperialist must be changed. To calculate the total authority of an empire, the percentage of the average authority of colonies and the imperialist of it is considered. The empires which cannot improve their authority in the imperialistic competition will gradually become weaker and will eliminate eventually. Therefore, their colonies will attach to other empires and stronger empires were created. The competition between the empires is done until only one empire remains. Finally, in this empire, the characteristic and authority of all the colonies and imperialist will be the same [42].

The steps of optimization process by ICA are as follows:

Step1- Produce initial country positions by Eq. (12).

$$X_{k,l}^{(0)} = U_{x_k}^b + rand.\left(U_{x_k}^b - L_{x_k}^b\right), \left| \begin{array}{l} k = 1,2, \dots, N_{DV} \\ l = 1,2, \dots, N \end{array} \right. \tag{12}$$

where $X_{k,l}^{(0)}$ is the initial value of the *k*th design variable for the *l*th country; $U_{x_k}^b$ and $L_{x_k}^b$ are side constraint; $rand$ is a random number between zero and one, N and N_{DV} are total number of countries and design variables respectively.

Step 2: Determine imperialist and colonies

After objective function of initial countries are computed, the empires are created. So, some of the countries with the high authority will be selected as the imperialist states and the rest of them will be the colonies.

Step 3- Move the colonies toward its related imperialists

The colony movement towards the imperialist was determined as Eq. (13):

$$\{X\}_{new} = \{X\}_{old} + U(0, \beta \times d) \times \{V_1\} \tag{13}$$

where U has a random cost that is distributed evenly between zero and $\beta \times d$. d and β are the distance between imperialist and colony and a scaler parameter that greater than 1 respectively. $\{V_1\}$ is a unit vector between the positions of the colony and the related imperialist.

The random parameter θ is considered to the direction of movement for expanding the searching space around the imperialist.

$$\theta = U(-\gamma, +\gamma) \tag{14}$$

where γ is a parameter that modifies the change from the main direction.

Step 4- Change of the position of the best colony and its imperialist

In this step, if a colony is produced with more than the associated imperialist, the position of the imperialist and colony will be changed.

Step 5: Calculate the total authority of an empire

The total of an empire is calculated based on both authority of the imperialist and its colonies as Eq. (15).

$$TC_l = f^{(imp,l)} + \xi . \frac{\sum_{i=1}^{NC_l} f^{(col,l)}}{NC_l} \tag{15}$$

where TC_l is the total authority of the *l*th empire, f is objective function, NC_l is the number of empires, ξ has a nonnegative value and less than one.

Step 6: Select the weakest colony in the least powerful empire and add it to the strongest empire.

Step 7: Decompose of the empires without colonies

Step 8: Stop the optimization procedure if the stop criteria are satisfied otherwise return to step 2.

The flowchart of ICA is proposed in Fig. 3 [42]. A complete explanation of how to apply the problem constraints during the optimization process is provided in reference [43].

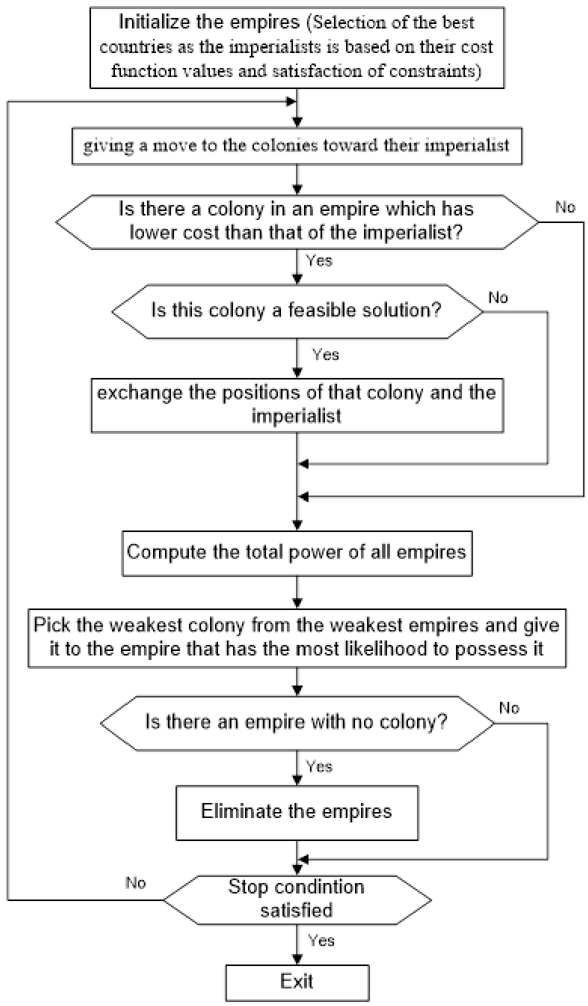

Figure 3. Flowchart of the imperialist competitive algorithm [42]

3.2 Imperialist competitive ant colony optimization

The main weakness of ICA is not balancing between exploration and exploitation phases in optimization steps [39]. In order to resolve this shortcoming, the two methods ICA and Ant Colony Optimization (ACO) were combined and a new hybrid method called imperialist competitive ant colony optimization (ICACO) was invented.

In ICACO, at first, initial ants (N_{Col}) are created. The positions of these ants are produced around their associated imperialist.

$$Ant_{l,n}^{k} = N(imp_N, \sigma), \left| \begin{array}{l} l = 1,2,\dots,N.C_n \\ n = 1,2,\dots,N_{imp} \end{array} \right. \tag{16}$$

where $N.C_n$ and N_{imp} are the number of colonies of the *n*th empire and imperialist respectively. The solution $Ant_{l,n}^k$ is produce by ant *l*th in empire *n*th in the iteration *k*;

$$Ant^k = \left[Ant_{1,1} \dots Ant_{N.C_1,1}\, Ant_{1,2} \dots Ant_{N.C_1,2} \dots Ant_{N.C_{imp},N_{imp}}\right]^T, \tag{17}$$

$$N.C_1 + N.C_2 + \cdots + N.C_{N_{imp}} = N_{col} \tag{18}$$

$N(imp_N, \sigma)$ has a normal random value that distributed with variance σ and average value imperialist *n*th. Variance σ is determined by Eq. (19).

$$\sigma = (U^b - L^b) \times \eta \tag{19}$$

Where L^b and U^b are the lower and upper bound respectively. η is applied to regulate the move step which initially is equal to one and by approaching to the optimum point, decreases gradually and finally tends to zero.

After producing Ants, the value of objective function of them ($f(Ant_{l,n}^k)$) is calculated. If $f(colony_{l,n}^k)$ is in the feasible domain and it is more than $f(Ant_{l,n}^k)$, the position of ant *l*th in empire nth ($Ant_{l,n}^k$) is changed with the position $colony_{l,n}^k$ (the current position of colony *l*th in empire *n*th).

The hybridization of ant colony optimization and imperialist competitive algorithm creates a balance between the exploration and the exploitation. Fig. 4 shows the flowchart of ICACO algorithm [39].

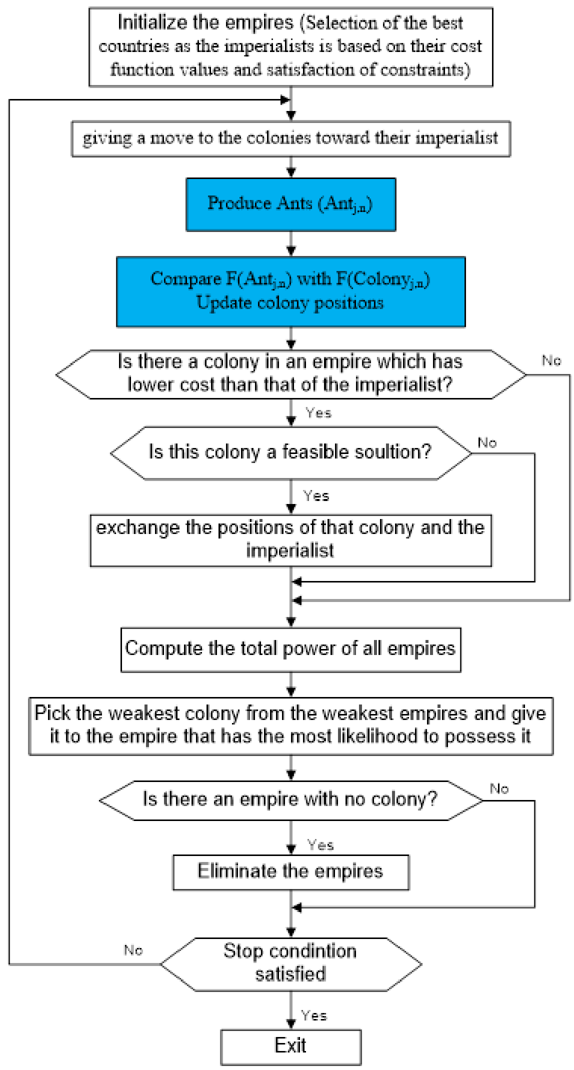

Figure 4. Flowchart of the imperialist competitive ant colony optimization [39]

4. OPTIMIZATION

A code is programmed in MATLAB to analyze the equations of motions. First, by using Eqs. (3) and (4) and initial conditions, the location of each auxiliary mass and sidewalls of the container are calculated. Then the collision condition is evaluated at each instance using Eqs. (8) and (9). If there is a collision, by using Eq. (10) and Eq. (11), new velocities are obtained. This procedure continues until the solution time is finished.

The sample response and the amplitude of the system with the conventional design of the impact damper are presented in Figs. 5 to 7 for parameters that are given in Table 1. For better view of the collisions between the damper mass and sidewalls, part of Fig. 5 is magnified.

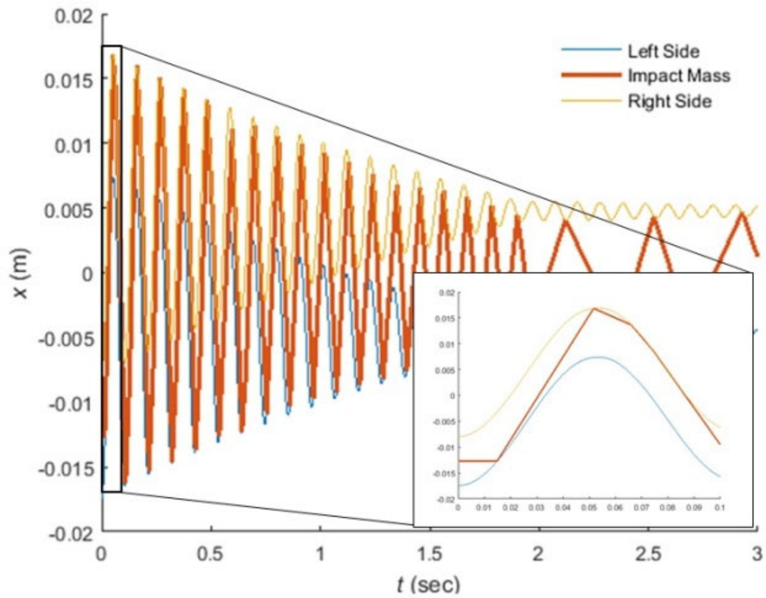

Figure 5. Time response of the system and the impact mass in the impact damper (conventional design)

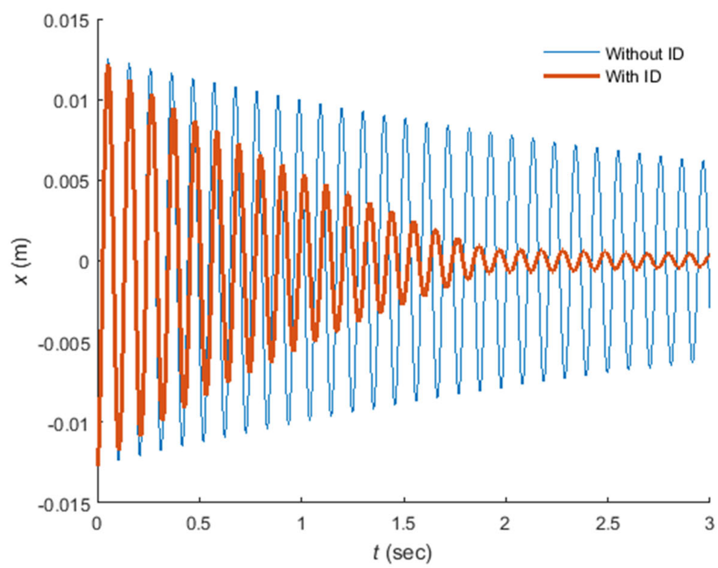

Figure 6. Time response of the system with and without the impact damper (conventional design)

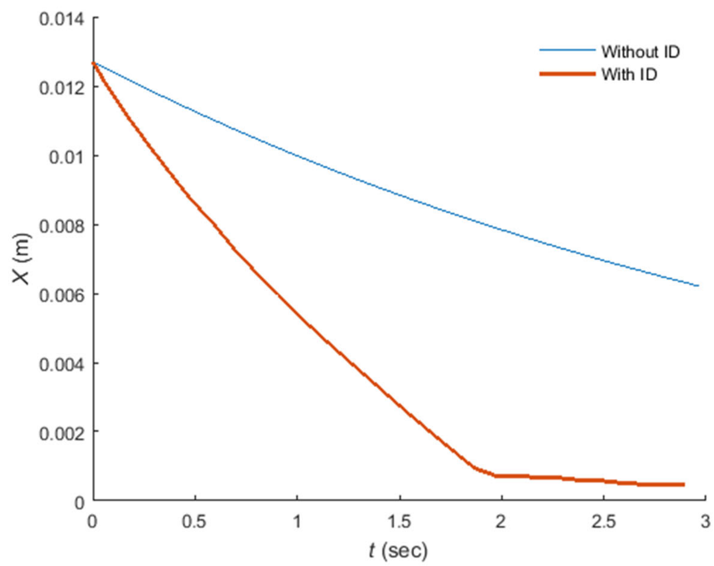

Figure 7. The Amplitude of the system with and without the impact damper (conventional design)

As shown in Figs. 5, 6, and 7, the behavior of impact damper can be classified into three zones. In the first zone, from 0 to 1.8 seconds, nearly, the impact mass has effective collisions with primary mass. This zone is named the impact zone. The effect of friction and structural damping is insignificant in the impact zone. In this zone, the decreasing rate of the amplitude of the position of the primary mass is nearly linear. This decreasing rate is named the damping inclination (DI).

In the second zone, from 1.8 to 2.7 seconds, nearly, the collisions between the impact mass and two end stoppers are not so effective. The reason for the movement of the impact mass in this zone is mainly the friction between the impact mass and the primary mass. This zone is named the friction zone. In the third zone, after 2.7 seconds, the movement of the impact mass relative to the primary mass is nearly insignificant. In this zone, the dynamic behavior of the system is similar to the system without impact damper. This zone is named the no-impact zone.

The velocity of main mass and impact mass in the system with the impact damper in conventional design is shown in Fig. 8.

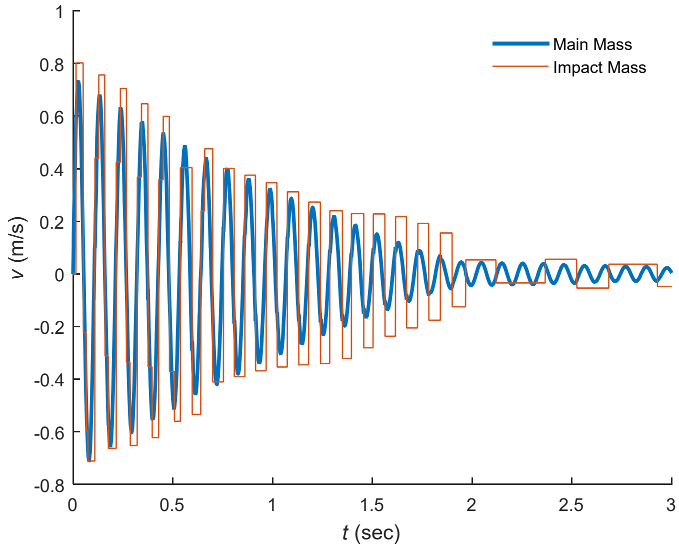

Figure 8. Velocity of the system and the impact mass in the impact damper (conventional design)

As shown in Fig. 8, the variation in the velocity of the impact mass is significant, so the impact damper is effective in vibration reduction of the main mass.

In this paper, the optimum design of the impact damper is performed by determining the optimum values of mass ratio ($\mu = m/M$), gap distance (d), and coefficient of restitution (e). The objective function (RDE) is the reduction percentage of the system energy as follows:

$$RDE = \frac{TE_D - TE_{WD}}{TE_{WD}} \times 100 \tag{20}$$

where TE_{WD} and TE_D are the total energy of the system without and with impact damper respectively. The limits of design parameters in the optimization problem are selected such that the design will be practical. For example, rational upper and lower limits are considered for the design variables to achieve a practical design in the optimum state.

Table 2 gives the results of the optimization using ICACO method. The bar diagram related to the design variables is shown in the lower part of Fig. 9. The upper part of Fig. 9 shows the convergence curve toward the optimum design. The blue and red curves correspond to the average and the best result at each iteration, respectively. The minus symbol indicates energy reduction. As shown in the upper part of Fig. 9, more than %94 of the system energy can be damped with the optimum design, relative to the system without impact damper.

The optimization method achieved the optimal design in less than 10 iterations and the two curves coincide in less than 45 iterations. After 45 iterations, only one empire exists in the population and power of all colonies and the empire becomes the same.

Table 2: Optimal design variables of single-mass impact damper

Design Variables	Value
μ (kg/kg)	0.019914
d (m)	0.002926
e	0.003234
RDE	-94.304493

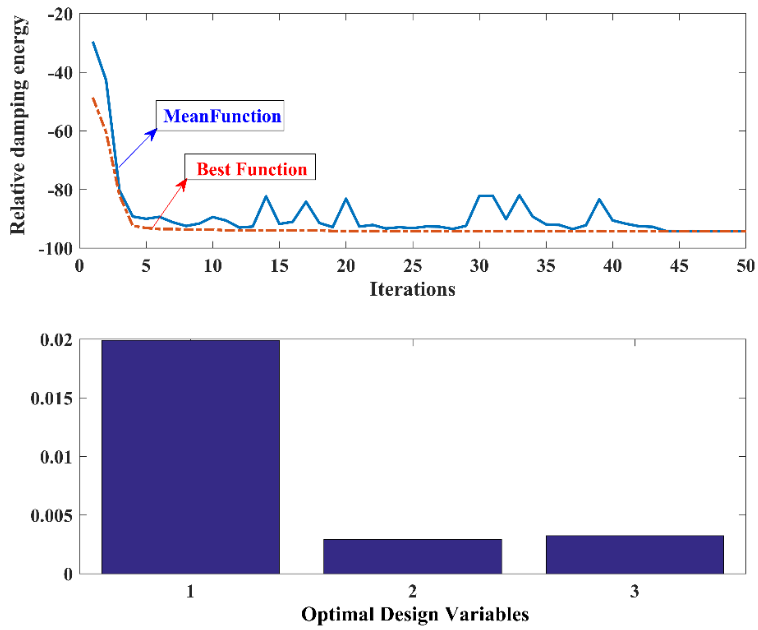

Figure 9. The convergence rates of relative damping energy and optimal design variables by ICACO

The time response and the amplitude of the system with optimized design of the impact damper are presented in Figs. 10 and 11 for parameters that are given in Table 2.

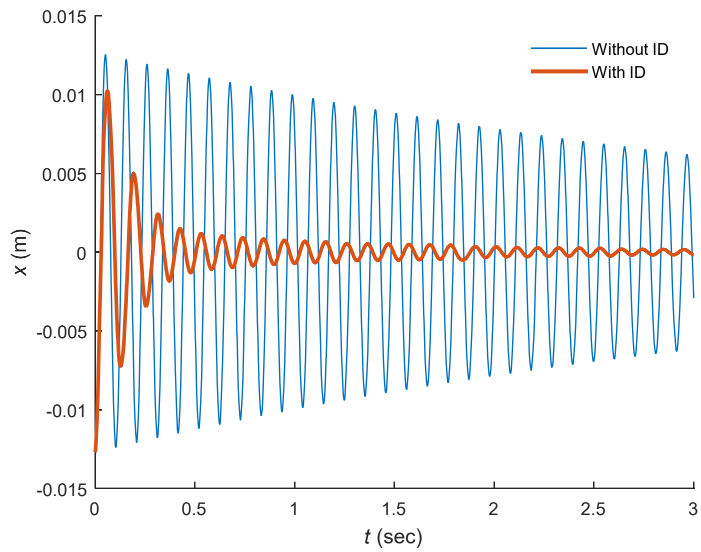

Figure 10. Time response of the system with and without the impact damper (optimized design)

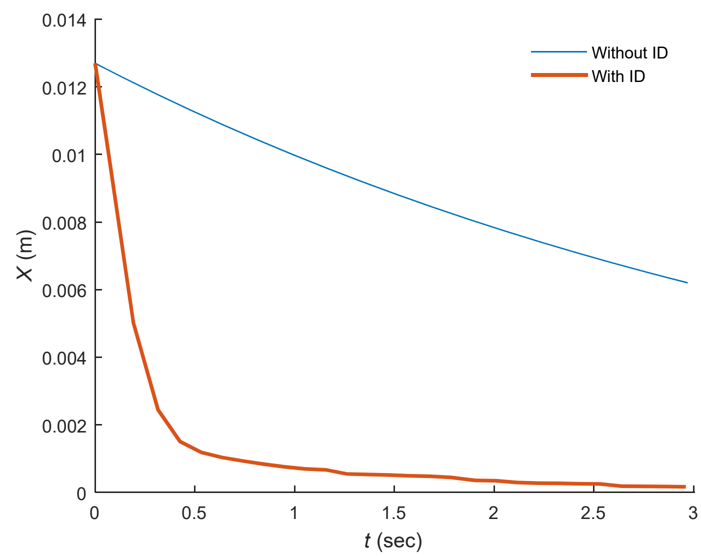

Figure 11. The Amplitude of the system with and without the impact damper (conventional design)

Comparing Figs. 10 and 11 with Figs. 6 and 7 show that the effect of the optimized impact damper on vibration reduction is much better than the conventional design. For better explanation, the percentage of energy damping of the main system in the conventional and the optimized impact dampers can be seen in Fig. 12.

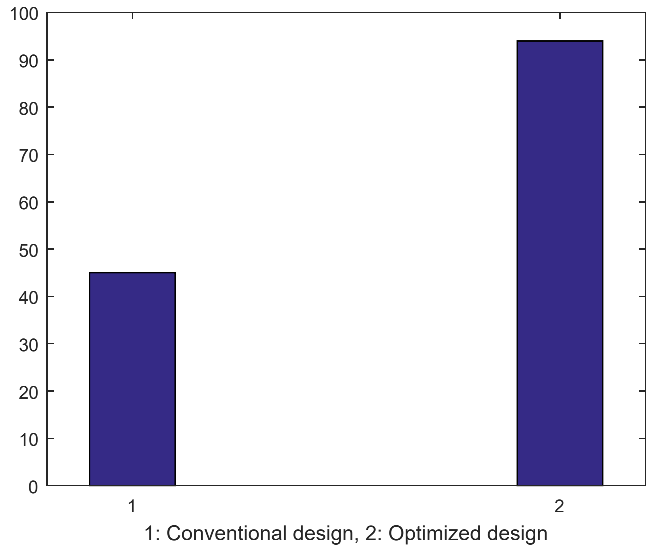

Figure 12. Energy damping percentage using impact damper (conventional and optimized design)

5. CONCLUSIONS

The behavior of impact damper can be classified into three zones. In the first zone, impact zone, the impact mass has effective collisions with primary mass. In the second zone, friction zone, the collisions between the impact mass and two end stoppers are not so effective. In the third zone, no-impact zone, the movement of the impact mass relative to the primary mass is nearly insignificant. In order to operate at maximum efficiency, the damper should be attached to the primary system at the point of maximum displacement. The performance of the impact damper depends on various parameters such as mass ratio, gap distance, and coefficient of restitution. Better performance of impact dampers occurs when the damper is placed away from the nodes of the mode shapes. That means better damping occurs when the damper is subjected to greater vibrations. The mass and packing ratios and distance of particle dampers are always important, but it is not always clear how they influence performance.

In this research, the optimal design of the impact damper parameters including the mass ratio, gap distance, and coefficient of restitution in free vibration of an SDOF system is performed. For the validation, the results of the single-mass damper are compared with those reported in the literature, and a good agreement is obtained. The optimum design is performed based on the maximum energy reduction of the primary system. The combinatorial and powerful optimization ICACO is used in this paper due to the complexity of the problem and calculations. The convergence rate is increased using this method, which provides achieving better results. The applicability of the results is also considered. The energy damped using the final optimum design is increased more than %94 relative to the initial design with no impact damper.

Acknowledgment: The authors wish to express appreciation to Education and Research Deputy of Bozorgmehr University of Qaenat for supporting this article by grant No. 39207.

REFERENCES

1. Lu Z, Wang ZX, Masri SF, Lu XL. Particle impact dampers: past, present, and future, *Struct Control Health Monitor* 2018; **25**: 1-25.
2. Vinayaravi R, Kumaresan D, Jayaraj K, Asraff AK, Muthukumar R, Experimental investigation and theoretical modelling of an impact damper, *J Sound Vib* 2013; **332**: 1324–34.
3. Yao B, Chen Q, Xiang HY, Gao X. Experimental and theoretical investigation on dynamic properties of tuned particle damper, *Int J Mech Sci* 2014; **80**: 122–30.
4. Blazejczyk-Okolewska B. Analysis of an impact damper of vibrations, *Chaos Soliton Fractal* 2001; **12**(11): 1983-8.
5. Shinde VL, Pathak AK, Review on particle damping technique for vibration suppression, *Int J Innovat Res Sci Eng Tech* 2016; **5**(3): 2890-5.
6. Safaeifar H, Farshidianfar A. Theoretically and parametrically investigation on operation of variable diameter impact damper in free vibrations of a 1-DOF system, *J Solid Fluid Mech* 2019; **9**(1): 15-26.
7. Zheng L, Kun L, Yuting O, Jiazeng Sh. Performance-based optimal design of tuned impact damper for seismically excited nonlinear building, *Eng Struct* 2018; **160**: 314-27.
8. Duncan MR, Wassgren CR, Krousgrill CM, The damping performance of a single particle impact damper, *J Sound Vib* 2005; **286**: 123-44.
9. Zheng L, Masri SF, Xilin L. Optimization Design of Impact Dampers and Particle Dampers, Particle Damping Technology Based Structural Control, 2020 (Book Chapter).
10. Afsharfard A, Farshidianfar A, Free vibration analysis of nonlinear resilient impact dampers, *Nonlin Dyn* 2013; **73**: 155-66.
11. Flores P, Machado M, Silva MT, Martins JM, On the continuous contact force models for soft materials in multibody dynamics, *Multibody Sys Dyn* 2011; **25**(3): 357-75.
12. Hu S, Guo X, A dissipative contact force model for impact analysis in multibody dynamics, *Multibody Sys Dyn* 2015; **35**(2): 131-51.
13. Safaeifar H, Farshidianfar A, A new model of the contact force for the collision between two solid bodies, *Multibody Sys Dyn* 2020; **50**(3): 233-57.
14. Michon G, Almajid A, Aridon G. Soft hollow particle damping identification in honeycomb structures, *J Sound Vib* 2013; **332**(3): 536–544.
15. Xia Z, Liu X, Shan Y, Li X. Coupling simulation algorithm of discrete element method and finite element method for particle damper, *J Low Frequency Noise Vib Activ Control* 2009; **28**(3): 197–204.
16. Xu Z, Wang MY, Chen T. Particle damping for passive vibration suppression: numerical modelling and experimental investigation, *J Sound Vib* 2005; **279**(3): 1097–1120.
17. Wang X, Liu X, Shan Y, He T. Design, simulation and experiment of particle dampers attached to a precision instrument in spacecraft, *J Vib Eng* 2015; **17**(4): 1605-14.
18. Lu Z, Lu X, Jiang H, Masri SF. Discrete element method simulation and experimental validation of particle damper system, *Eng Comput* 2014; **31**(4): 810-23.

19. Ibrahim R. *Vibro-impact Dynamics: Modeling, Mapping and Applications*, Springer, Verlag Berlin Heidelberg, 2009.
20. Gagnon L, Morandini M, Ghiringhelli GL. A review of particle damping modeling and testing, *J Sound Vib* 2019; **459:** 114865.
21. Masri SF. Analytical and Experimental Studies of Impact Dampers. Ph.D. Thesis, California Institute of Technology 1965.
22. Masri SF. Analytical and experimental studies of multiple-unit impact dampers, *J Acoust Society America* 1969; **45**(3): 1111-17.
23. Masri SF. Steady-State Response of a Multidegree System with an Impact Damper, *J Appl Mech* 1973; 27-132.
24. Bapat CN, Sankar S. Single Impact Damper in Free and Forced Vibration, *J Sound Vib* 1985; **99**(1): 85-94.
25. Ema S, Marui E. A fundamental study on impact dampers, *Int J Mach Tools Manuf*act 1994; **34**(3): 407-421.
26. Afsharfard A, Kolahan F. Reliability-based design for damping behavior of inner mass single-unit impact dampers, *Quality Reliab Eng Int* 2013; **29**: 521-7.
27. Xiaowei L, Yue Y, Weixing Sh. Study on the Damping Effect of Particle Dampers considering Different Surface Properties, *Shock Vib* 2019; Article ID 8293654.
28. Zurawski M, Zalewski R. Damping of Beam Vibrations Using Tuned Particles Impact Damper, *Appl Sci* 2020; **10**(18), 6334.
29. Osman OE, Stefan H. Application of an SMA-based hybrid control device to 20-story nonlinear benchmark building, *Earthquak Eng Struct Dyn* 2012; **41**(13): 1831–43.
30. Rana R, Soong TT. Parametric study and simplified design of tuned mass dampers, *Eng Struct* 1998; **20**(3):193–204.
31. Bakre SV, Jangid RS. Optimal parameters of tuned mass damper for damped main System, *Struct Control Health Monitor* 2007; **14**(3): 448–70.
32. 32. Hadi MNS, Arfiadi Y. Optimum design of absorber for MDOF structures, *J Struct Eng ASCE* 1998; **124**(11): 1272–80
33. Leung AYT, Zhang H. Particle swarm optimization of tuned mass dampers, *Eng Struct* 2009; **31**(3): 715–28.
34. Steinbuch R. Bionic optimization of the earthquake resistance of high buildings by tuned mass dampers, *J Bionic Eng* 2011; **8**(3): 335–44.
35. Jin Ch, Chung Ch, Kwon D, Kim, M. Optimization of tuned mass damper for seismic control of submerged floating tunnel, *Eng Struct* 2021; **241**: 112460,
36. Bekdas G, Nigdeli SM. Estimation optimum parameters of tuned mass dampers using harmony search, *Eng Struct* 2011; **33**(9): 2716–23.
37. Lara-Valencia LA, Caicedo D, Valencia-Gonzalez Y. A novel whale optimization algorithm for the design of tuned mass dampers under earthquake excitations, *Appl Sci* 2021; **11**(13): 6172.
38. Ghoddosian A, Sheikhi Azqandi M. *Metaheuristic Optimization Algorithm in Engineering*, Semnan University Press, 2013.
39. Sheikhi M, Ghoddosian A. A hybrid imperialist competitive ant colony algorithm for optimum geometry design of frame structures, *Struct Eng Mech* 2013, **46**(3): 403-16.
40. Rao SS. *Mechanical Vibrations*, 6th ed in SI Units, Pearson, 2018.

41. Meriam JL, Kraige LG, Bolton JN. *Engineering Mechanics Dynamics*, 8th ed, Wiley, 2015.
42. Sheikhi M, Nooredin N, Ghoddosian A. Optimization of spring back in U-die bending process of sheet metal using ANN and ICA, *Struct Eng Mech* 2018; **65**(4): 447-52.
43. Ghoddosian A, Eskandar H, Sheikhi Azqandi M. Optimal design of vessels by using imperialist competitive algorithm, *J Appl Comput Sci Mech* 2013; **25**(1): 125-34.